Free Carrier Screening in Coupled Asymmetric GaN Quantum Discs

K.H. Lee[a], J.H. Na[a], S. Birner[b], R.A. Taylor[*a], S.N. Yi[a], Y.S. Park[c], C.M. Park[c], and T.W. Kang[c]

[a] Department of Physics, University of Oxford, Parks Road, Oxford, OX1 3PU, United Kingdom
[b] Walter Schottky Institute and Physics Department, Technical University of Munich, D-85748 Garching, Germany
[c] Quantum-functional Semiconductor Research Center, Dongguk University, Seoul 100-715, South Korea

ABSTRACT

We present an investigation of free-carrier screening in coupled asymmetric GaN quantum discs with embedded AlGaN barriers using time-integrated and time-resolved micro-photoluminescence measurements, supported by three-dimensional multi-band **k.p** computational modeling. We observe that with increasing optical excitation the carrier lifetime decreases and emission energy blue-shifts. This originates from the screening of built-in piezo- and pyroelectric fields in the quantum discs by photo-generated free-carriers. Due to non-resonant tunneling of carriers from the smaller disc to the larger disc, free carrier screening is enhanced in the larger disc. The non-resonant tunneling was found to have a significant role in samples with a thin barrier, as the screening decreased with barrier thickness (i.e. decreased tunneling). Computational modeling was in good agreement with the experimental results.
Keywords: Photoluminescence, Quantum effect semiconductor devices, Free-carrier screening

1 INTRODUCTION

Low dimensional nitride-based semiconductors incorporating quantum wells (QWs) and quantum dots (QDs) have attracted much attention due to their application in blue/ultra-violet wavelength optoelectronic devices[1]. In particular, self-organized GaN nanocolumns have gained interest as they possess desirable properties such as low defect density, good reproducibility, quantum confinement effects[2] and can be produced using conventional growth techniques without additional processing. These properties make nanocolumns an attractive basis for future quantum optoelectronic devices (such as embedded QDs in nanopillar cavities for quantum information processing[2]). Significant advancements has been made towards practical devices, with GaN nanocolumn experiments employing Bragg reflectors[3], electrical excitation[4] and stimulated emission[5] having been undertaken. QW like structures grown at the tip of GaN nanocolumns are known as quantum discs (Q-discs) and demonstrate lateral confinement. We have investigated coupled asymmetric GaN Q-discs separated by thin AlGaN barriers, as carrier tunneling in such structures has been suggested previously[6] and could play a role in future devices.

In this paper we present measurements and analysis of free-carrier screening and optical nonlinearity in a III-nitride Q-disc structure, with an enhancement in the emission from the larger Q-disc due to carrier tunneling. We have examined these effects using a combination of time-resolved (TR-) and time-integrated (TI-) photoluminescence (PL) spectroscopy and multi-band **k.p** computational modeling with next**nano**^{3} [7]. From the TI- and TR-PL measurements we observe that increased optical excitation leads to a reduction in the lifetime and blue-shift in the emission, with the effect being more pronounced in the larger Q-disc due to carrier tunneling.

* r.taylor1@physics.ox.ac.uk; phone: (01865) 272-230

Optoelectronic Materials and Devices, edited by Yong Hee Lee, Fumio Koyama, Yi Luo,
Proc. of SPIE Vol. 6352, 635214, (2006) · 0277-786X/06/$15 · doi: 10.1117/12.689176

2 SAMPLE DETAILS

The GaN/AlGaN Q-discs were grown at the tip of a 2.7-µm-high GaN nanocolumn using plasma assisted molecular beam epitaxy on a Si (111) substrate without any buffer layer[8]. The growth of GaN nanocolumns was performed under N-rich conditions. The Ga flux was controlled to a beam equivalent pressure of 2×10^{-7} Torr, which was approximately ten times smaller than that used for GaN epilayers (4×10^{-6} Torr). The power and flow rate of the N plasma source were 350 W and 2.0 sccm, respectively. A growth temperature of 750 °C was used. The Al mole fraction of the AlGaN barrier was deduced by means of a linear interpolation of Al content determined by high resolution x-ray diffraction as a function of Al cell temperature in the limit of nanocolumns. Cross-sectional and plan view SEM images of the nanocolumns are depicted in Figs. 1(a-b). The hexagonal GaN nanocolumns exhibited various diameters ranging from 50 to 120 nm and a density of 1×10^{9} cm^{-2}. The Q-disc sample consisted of ten periods of two alternating GaN Q-disc thicknesses of 4 and 3 nm, separated by an $Al_{0.5}Ga_{0.5}N$ barrier with an effective thickness of 1 nm. The larger Q-disc was referred to as DA, while the smaller Q-disc was referred to as DB [Fig 1(c)].

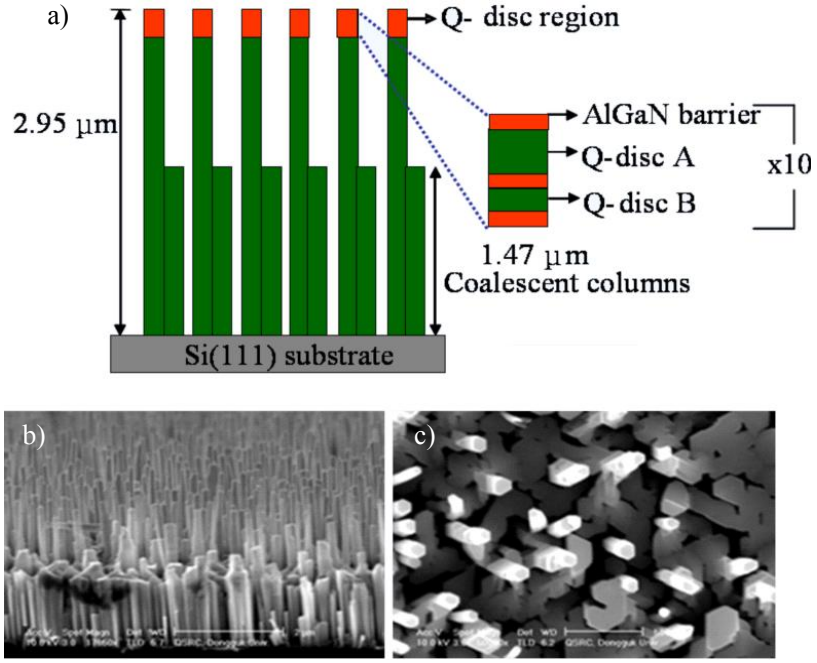

Fig. 1. (a) Schematic diagram of the Q-disc sample. (b) Cross-sectional and (c) plan view SEM images of the sample, showing the hexagonal columnar structure. The GaN Q-discs are embedded at the top region of the nanocolumn sample.

3 COMPUTATIONAL MODELING

This structure was investigated by next**nano**[3], a nanostructure simulator capable of solving the self-consistent 3D nonlinear Poisson-Schrödinger equation for wurtzite materials including strain, deformation potentials and piezo- and pyroelectric charges. For the calculations, we employed the material parameters taken from Ref. 9. The fully strained Q-discs were simulated by minimization of the elastic energy within a continuum model approach that takes into account the symmetry of the hexagonal crystal structure. For the air-semiconductor interface we assumed that the atoms at the GaN boundary of the Q-disc were not allowed to relax into the surrounding air material. In order to calculate the wavefunctions a single-band model for the electrons and a six-band k.p Hamiltonian for the holes were considered. This could be justified as GaN and AlN have large band gaps and therefore the coupling between the conduction and valence bands can be neglected for our purpose[10].

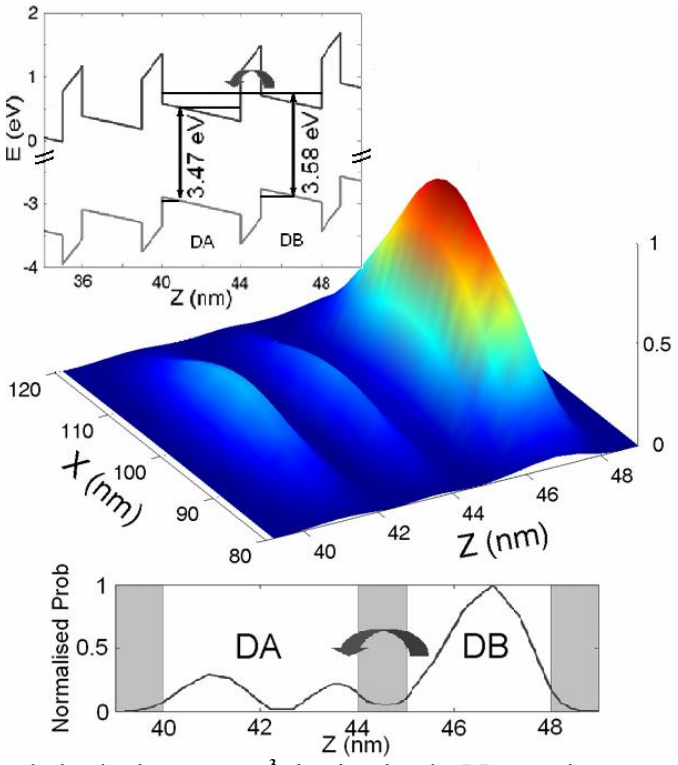

Fig. 2. Electron wavefunctions calculated using next**nano**[3] showing that the DB ground state extends into DA, giving rise to the possibility of tunneling from DB to DA. Band diagram for electrons and holes with the energy levels labeled (inset).

Figure 2(a) shows a visualization of the conduction and heavy hole valence band along the growth direction (i.e. c-axis [0001]). Wurzite III-nitride heterostructures have a built-in piezo- and pyroelectric field (~several MV/cm) which tilts the bands, giving rise to a quantum confined Stark effect (QCSE) for the carriers. This results in a red-shift and the spatial separation of the confined electrons and holes. The calculated energy levels for the electrons and holes and the DA and DB emission energies are also presented in Fig. 2(inset). The emission energies from DA and DB were calculated to be 3.47 and 3.58 eV, respectively. The calculations show that the tunneling of electrons from DB to DA is possible, as the electron energy of DB lies above the triangular potential of the DA energy state. However, the converse is not true as the electron energy in DA was lower (by ~0.1 eV) and the energy of the electron lies within the triangular region of potential, implying stronger localization. The effect of tunneling was investigated by considering the squared wavefunctions that were obtained as the solutions of the Schrödinger equation, which was solved for the three-dimensional region that includes both Q-discs. Figure 2 shows that the probability density for the ground state of the electron in DB tunnels through the AlGaN barrier and extends into DA. Hence, even under non-resonant condition, there is evidence of weak coupling between the Q-discs.

4 EXPERIMENTAL RESULTS

4.1 Experimental Setup

TI-PL and TR-PL measurements were undertaken in order to look for the effects of the predicted tunneling. For these measurements, frequency-tripled femtosecond Ti:sapphire laser pulses at 266 nm were used for excitation. These pulses had duration 150 fs and a repetition frequency of 76 MHz (Coherent MIRA). The sample was mounted in a continuous-flow helium cryostat (Janis ST-500) and the temperature was maintained at 4 K. A 36× reflecting objective (Ealing) was held above the cryostat to both focus the incident laser beam to a spot size of ~2 μm and to collect the resulting luminescence. The PL was dispersed by a 0.3 m spectrograph, which was equipped with a 1200 grooves/mm grating giving a spectral resolution of ~0.7 meV. For TI measurements the PL was detected by a Peltier-cooled CCD, and for TR measurements the PL was directed to a commercial time-correlated single photon counting system with a rise-time of 50 ps.

4.2 TI-PL

Optical nonlinearities in the Q-disc were investigated using TI-PL. Spectra as a function of excitation power ranging from 10 μW to 1.2 mW (at the focus) are presented in Fig. 3. Two peaks were observed at 3.48 and 3.56 eV, labeled DA and DB in the spectra. These were in good agreement with the calculated values (3.47 and 3.58 eV). As the excitation power increased the DA peak grew more rapidly, relative to DB peak, and it eventually dominated the spectra. This is reflected in the peak intensity versus excitation power plot (Fig.3 inset), which showed that the DB peak intensity was proportional to the excitation power, while the DA peak intensity displayed a nonlinear dependence with excitation power. This observation is consistent with earlier studies involving GaAs/AlGaAs asymmetric QWs, which demonstrated nonlinear PL dependence with excitation power, due to carrier tunneling[11].

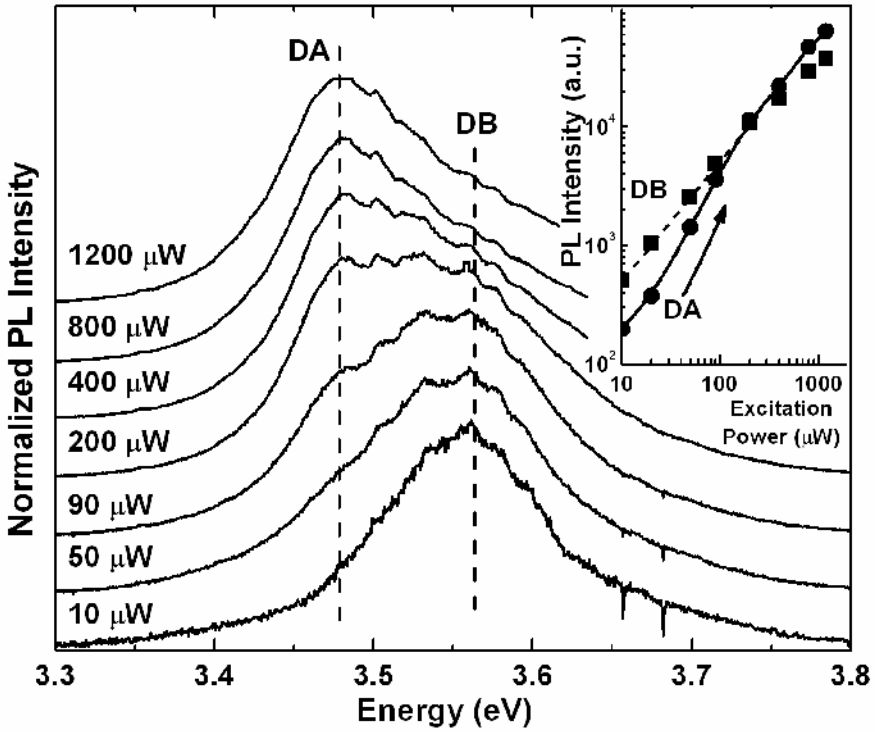

Fig. 3. Normalized TI-PL spectra of the GaN Q-discs. Inset shows a plot of peak intensity versus excitation power.

4.3 TR-PL

Through TR-PL measurements, the effects of free-carrier screening were studied. Figure 4 shows the TR-PL trace collected from the DA and DB peaks, at high (600 μW) and low (40 μW) excitation power. The TR-PL traces show a single exponential decay at low excitation power, with fitted lifetimes of τ_{DA} = 460 ps for DA and τ_{DB} = 360 ps for DB. At high excitation power the TR-PL traces show a biexponential decay, with a fast component of τ_1 =100 ps, which was common to both DA and DB, and τ_{DA} = 300 ps and τ_{DB} = 300 ps. The fast component was identified with free carrier decay and screening, which has a more significant contribution with increasing optical excitation. The decrease in τ_{DA} and τ_{DB} with increasing optical excitation could be explained by free-carrier screening[12], which compensates the built-in piezo- and pyroelectric field (responsible for the QCSE). The photo-generated free-carriers screen the built-in fields, which then leads to a reduction in the band structure tilt and consequently the overlap between electron and hole increases, which corresponds to an increased oscillator strength (stronger peak intensity and decreased carrier lifetime).

Enhancement of the free-carrier screening due to tunneling was investigated by reconstructing the spectrum from a series of TR-PL measurements, which were performed at 0.02 eV intervals (from 3.44 to 3.64 eV) for an incident power of 600 μW, as shown in Fig. 5. The measured response displays several interesting features. Initially the DA and DB peaks are blue-shifted (3.50 and 3.60 eV) compared to TI-PL peaks. During the initial decay period (0-400 ps) DA peak blue-shifts linearly at 0.15 meV/ps while DB peak red-shifts and sharpens. This behavior arises from the transfer of electrons from

DB to DA (i.e. tunneling) and hence the DA electron population increases, leading to a blue-shift and decrease in the QCSE due to free-carrier screening. This phenomenon also corresponds to the transition region on the TR-PL curve for DA, at which the trace moves from the rapid to the slower decay characteristics. Between 400-700 ps the rate of tunneling decreases, with a reduced electron population in DB, and the carriers in DB and DA recombine (with a lifetime of ~300 ps). After 700 ps DA and DB experience a red-shift as the carriers further recombine, and hence the effect of the free-carrier screening is reduced. Here, the peak energies for DA and DB return to the values seen at low excitation. The peak observed at ~ 3.60 eV (labeled C) corresponds to the GaN nanocolumn[6]. Overall, this response is in good agreement with behavior observed in symmetric III-nitride QWs (e.g. InGaN/GaN)[13]. These measurements demonstrate that the free-carrier screening is enhanced in DA and agrees with predictions from TI-PL and computational modeling results. The dynamic response of the system explains why the DA blue-shift could not observed in the TI-PL spectrum, which is a summation of the PL slices in Fig. 5. Further studies reveal that this enhancement decreases as the barrier thickness increases (from 2 to 8 nm).

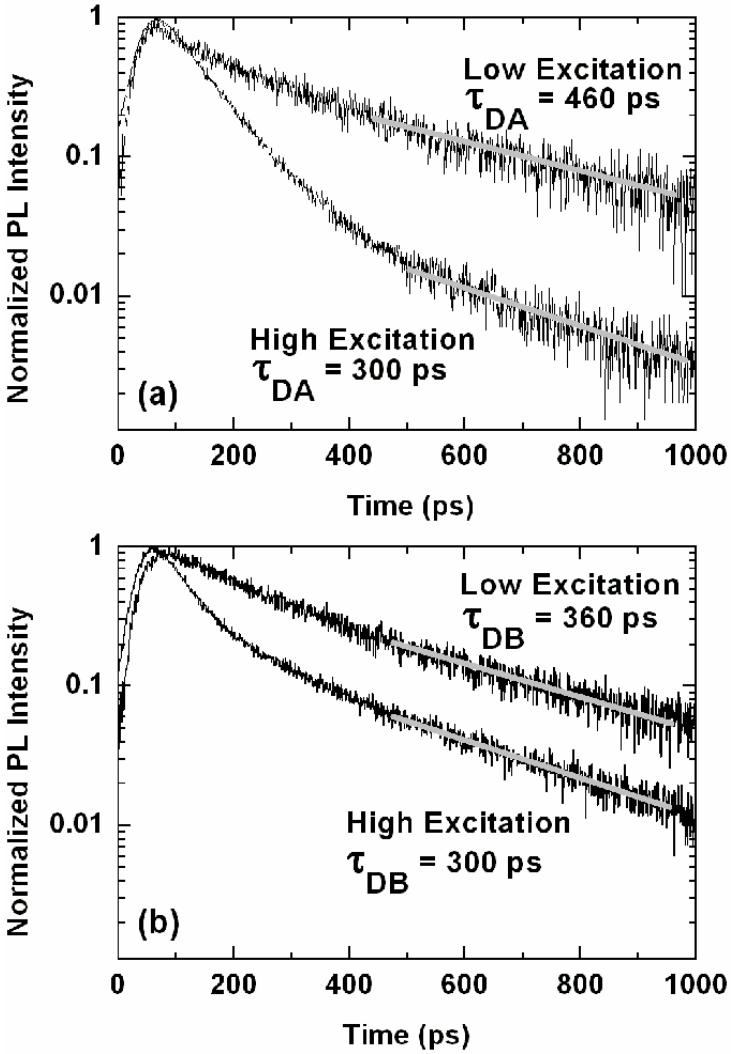

Fig. 4. TR-PL measurement from DA (a) and DB (b), at low and high excitation powers. The effect of the free-carrier screening can be seen, with the carrier lifetime decreasing with increasing optical power.

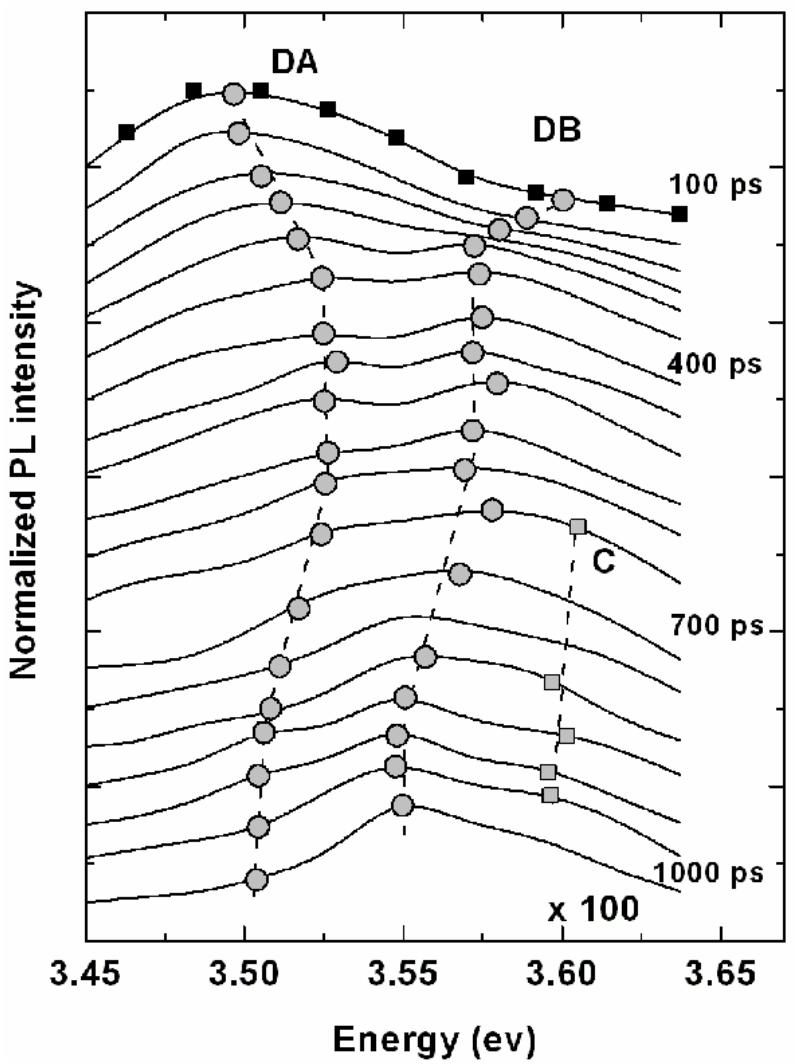

Fig. 5. Reconstruction of the spectrum from TR-PL measurements at an excitation powers of 600μW. The time increment between each line is 50 ps. Time origin as in Fig. 4.

4.4 Influence of Barrier Thickness

The influence of non-resonant tunneling on the free-carrier screening was studied[14] by growing new samples with the same geometry (4nm – DA and 3 nm – DB), but with varying $Al_{0.5}Ga_{0.5}N$ barrier thickness (2, 4 and 8nm).

Figure 6 shows the TI-PL spectra as a function of excitation power ranging from 20 μW to 1.4 mW (at the focus) for the sample with 2 and 8 nm barrier thickness. The 2 nm barrier sample displayed a behavior similar to the original sample (with 1 nm barrier); with the DB peak intensity proportional to the excitation power and DA peak intensity displaying a nonlinear dependence with excitation power. However, the DA peak nonlinearity was significantly reduced in the 8 nm sample. Figure 7 shows the TR-PL trace collected from the DA and DB peaks, at high (1.4 mW) and low (20 μW) excitation power for both 2 and 8 nm barrier samples. In the 2 nm barrier sample DA lifetime decreased from 530 to 240 ps (20 μW to 1.4 mW) while for the sample with the 8nm barrier, DA lifetime decreased from 510 to 400 ps (20 μW to 1.4 mW). Over this range DB lifetime only varied from 480 to 380 ps in both the 2 and 8 nm samples. Hence these results demonstrate that tunneling of carriers plays a significant role in the free-carrier screening.

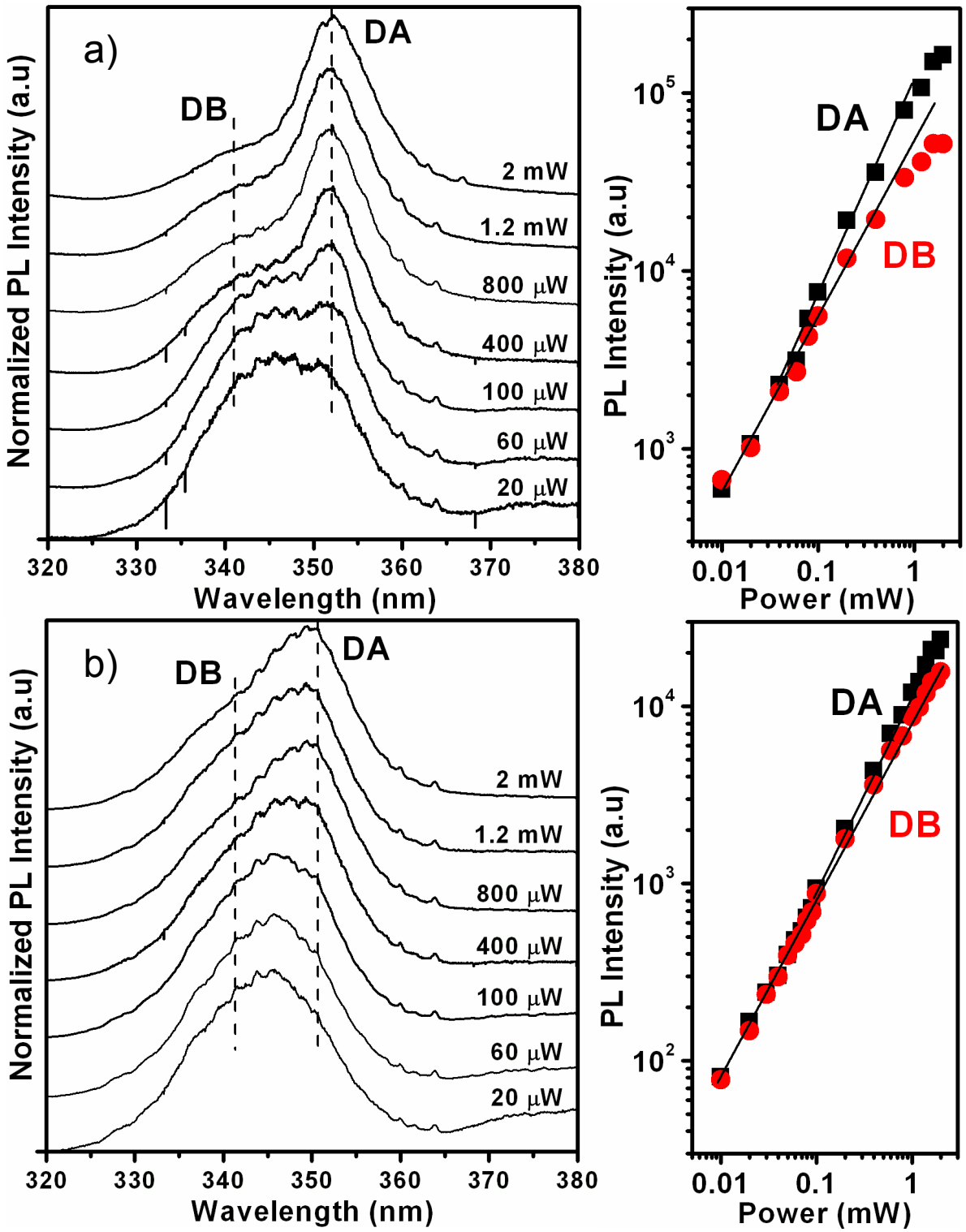

Fig. 6. Normalized TI-PL spectra and a plot of peak intensity versus excitation power for a Q-disc sample with 2 nm (a) and 8 nm (b). Nonlinear dependence is

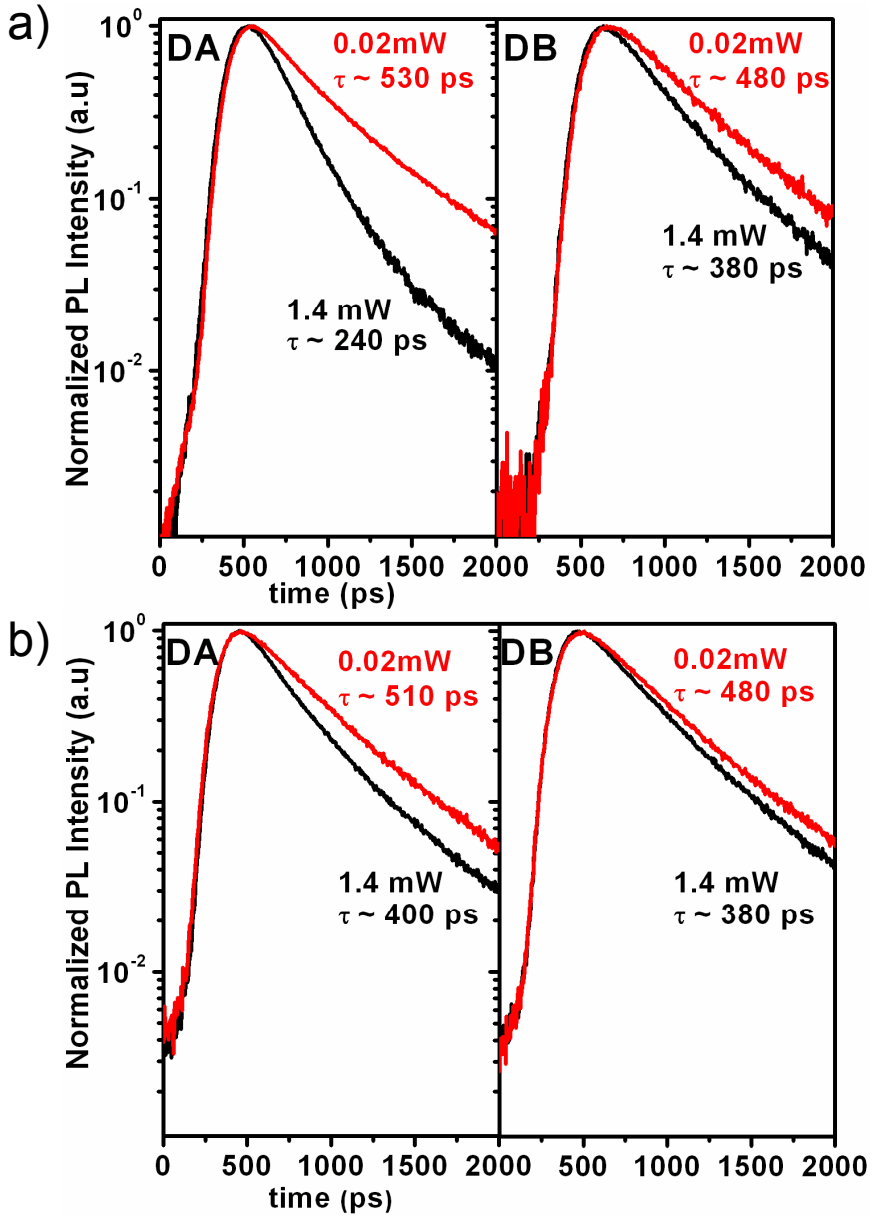

Fig. 7. TR-PL measurement from the sample with 2 nm (a) and 8 nm (b) thick barrier, at low and high excitation powers. The influence of the barrier thickness can be seen, with the carrier lifetime decreasing significantly in the sample with the thinner barrier..

5 CONCLUSION

In conclusion free-carrier screening in a coupled asymmetric Q-disc system has been investigated using a combination of TI-PL and TR-PL techniques, and next**nano**[3] multi-band **k.p** computational modeling. Due to the free-carrier screening of the built-in fields, carrier lifetime decreased with increasing optical excitation. This change was more pronounced in DA due to additional free carriers arising from tunneling of electrons from DB to DA. This was verified by further studies involving asymmetric GaN Q-disc samples with varying barrier thickness – which showed that the effects of screening decreased with increasing barrier thickness (i.e. reduction of the tunneling).

This research is part of the QIP IRC supported by EPSRC (GR/S82176/01). KHL thanks the support of the University College old members fund, Clarendon Fund bursary, Overseas Research Students award, Wingate Foundation and M.A.G. Jones for computational support. YSP, CMP and TWK thanks QSRC and AOARD at Dongguk University.

REFERENCES

[1] S. Nakamura, M. Senoh, S. I. Nagahama, N. Iwasa, T. Yamada, T. Matsushita, H. Kiyokyu and Y. Sugimoto, Jpn. J. Appl. Phys., **35**, L74 (1996).
[2] M. Zamfirescu, M. Abbarchi, M. Gurioli, A. Vinattieri, J. Ristić, and E. Calleja, phys. stat. sol. (c) **2**, 822 (2005).
[3] J. Ristić, E. Calleja, A. Trampert, S. Fernández-Garrido, C. Rivera, U. Jahn, and K. H. Ploog, Phys. Rev. Lett., **94**, 146102 (2005).
[4] A. Kikuchi, M. Kawai, M. Tada and K. Kishino, Jpn. J. Appl. Phys., **43**, L1524 (2004).
[5] A. Kikuchi, K. Yamano, M. Tada, and K. Kishino, phys. stat. sol. (b) **241**, 2754 (2004).
[6] J. H. Na, R. A. Taylor, J. H. Rice, J. W. Robinson, K. H. Lee, Y. S. Park, C. M. Park, and T. W. Kang, Appl. Phys. Lett., **86**, 083109 (2005).
[7] next**nano³** device simulator: The program is available at www.wsi.tum.de/nextnano3 and www.nextnano.de.
[8] C. M. Park, Y. S. Park, Hyunsik Im, and T. W. Kang, Nanotechnology 17, 952 (2006).
[9] I. Vurgaftman, J. R. Meyer, J. Appl. Phys., **94** (6), 3675 (2003).
[10] V. A. Fonoberov and A. A. Balandin, J. Appl. Phys., **94** (11), 7178 (2003).
[11] D. J. Leopold, M.M. Leopold, Phys. Rev. B, **42**(17), 11147 (1990).
[12] F.D. Sala, A. Di Carlo, P. Lugli, F. Bernardini, V. Fiorentini, R. Scholz, J.-M. Jancu, Appl. Phys. Lett., **74**(14), 2002 (1999).
[13] T. Kuroda, A. Tackeuchi and T. Sota, Appl. Phys. Lett., **76**(25), 3753 (2000).
[14] K.H. Lee et al., ICPS-28, Vienna, Austria, July 24-28, 2006